Journal of
Marine Science and Engineering

MDPI

Brief Report

Timescales of Magma Mixing Beneath the Iheya Ridge, Okinawa Trough: Implications for the Stability of Sub-Seafloor Magmatic Systems

Yuxiang Zhang [1,2,3,*], Zuxing Chen [1,2,3] and Zhigang Zeng [1,2,3,*]

[1] Seafloor Hydrothermal Activity Laboratory, CAS Key Laboratory of Marine Geology and Environment, Institute of Oceanology, Chinese Academy of Sciences, Qingdao 266071, China
[2] Laboratory for Marine Mineral Resources, Qingdao National Laboratory for Marine Science and Technology, Qingdao 266071, China
[3] Center for Ocean Mega-Science, Chinese Academy of Sciences, Qingdao 266071, China
[*] Correspondence: yxzhang@qdio.ac.cn (Y.Z.); zgzeng@qdio.ac.cn (Z.Z.)

Abstract: Submarine volcanic eruptions can be destructive for marine environments and resources. Magma mixing is considered to be an important trigger for volcanic eruptions. Determining the magma residence time from mixing to eruption is conducive to assessing the stability of magmatic systems, especially beneath the seafloor where in situ volcano monitoring is inaccessible. Here, we estimated the timescale of magma mixing beneath the Iheya Ridge, Okinawa Trough, which is characterized by pervasive magma mixing. We focused on andesitic and rhyolitic magma generated by basalt–rhyolite mixing and rhyolite–rhyolite mixing, respectively. By taking advantage of the Mg diffusion chronometry, we showed that the andesitic magma resided in the magma chamber for very short time (~0.1–0.3 years), whereas the residence time of the rhyolitic magma was much longer (~80–120 years). The different times might be in part related to the different rheology of the mixed magmas. The short residence time of the andesitic magma suggested efficient magma mixing that allowed the andesites to be erupted, which may explain the appearance of scarce andesites in basalt–rhyolite dominant settings. However, the rapid mixing and eruption of magma is a disadvantage for the development and preservation of seafloor hydrothermal resources. Therefore, we suggest that the stability of sub-seafloor magma systems must be evaluated during the assessment of seafloor sulfide resources and mining prospects.

Keywords: magma residence time; magma mixing; diffusion chronometry; magma eruption; seafloor hydrothermal activity

check for updates

Citation: Zhang, Y.; Chen, Z.; Zeng, Z. Timescales of Magma Mixing Beneath the Iheya Ridge, Okinawa Trough: Implications for the Stability of Sub-Seafloor Magmatic Systems. *J. Mar. Sci. Eng.* **2023**, *11*, 375. https://doi.org/10.3390/jmse11020375

Academic Editor: János Kovács

Received: 25 December 2022
Revised: 29 January 2023
Accepted: 30 January 2023
Published: 8 February 2023

1. Introduction

Sub-seafloor magma systems are huge energy reservoirs, which are not only the most important heat source for seafloor hydrothermal activities but can also supply volatiles and/or metals to hydrothermal systems [1–3]. However, submarine volcanic eruptions can be extremely destructive. For example, they can trigger serious natural disasters such as earthquakes and tsunamis [4,5]. In addition, huge amounts of heat and toxic gases emitted from the seafloor could have catastrophic impacts on marine environments and ecosystems [3,6]. Furthermore, they can also damage previously formed hydrothermal systems, which is a potential threat that should not be ignored in the assessment of seafloor sulfide resources and mining feasibility. Therefore, it is essential to evaluate the stability of sub-seafloor magma systems and assess the residence times of magmas prior to eruption.

While it is difficult to monitor magmatic activity beneath the seafloor in situ, the instabilities of a deep magma reservoir may be partly reflected by complex magmatic processes such as magma mixing, which can be recorded by the mineralogy of erupted lavas [7–12]. The timescales of magmatic processes can be estimated by diffusive re-equilibration within crystals [13–21].

The Okinawa Trough (OT) is a young back-arc basin that is characterized by complex volcanic systems, widespread seafloor hydrothermal systems, and extremely high heat flow values [22–24]. Widespread magma mixing is suggested to have occurred in the shallow magma chambers of the OT [25,26]. However, the timescales of magma mixing have not been well constrained. In this study, we focused on the magma system beneath the Iheya Ridge, where basalt–rhyolite mixing and rhyolite–rhyolite mixing have been recorded by the chemical zonation of minerals [26], and estimated the residence times of magmas from mixing to eruption using diffusion chronometry.

2. Geological Setting and Samples

The OT is located in the eastern margin of the East China Sea Shelf (Figure 1). It is a newly developed back-arc basin, and its initial extension can be traced back to the middle-to-late Miocene in response to the subduction of the Philippine Sea plate [27]. The OT is generally divided into three segments from the north to the south, namely the NOT, MOT, and SOT. Several central grabens, which represent the active back-arc spreading centers, have developed in the MOT and SOT. The SOT and MOT are also characterized by widespread hydrothermal activities and complex volcanic systems [23,28].

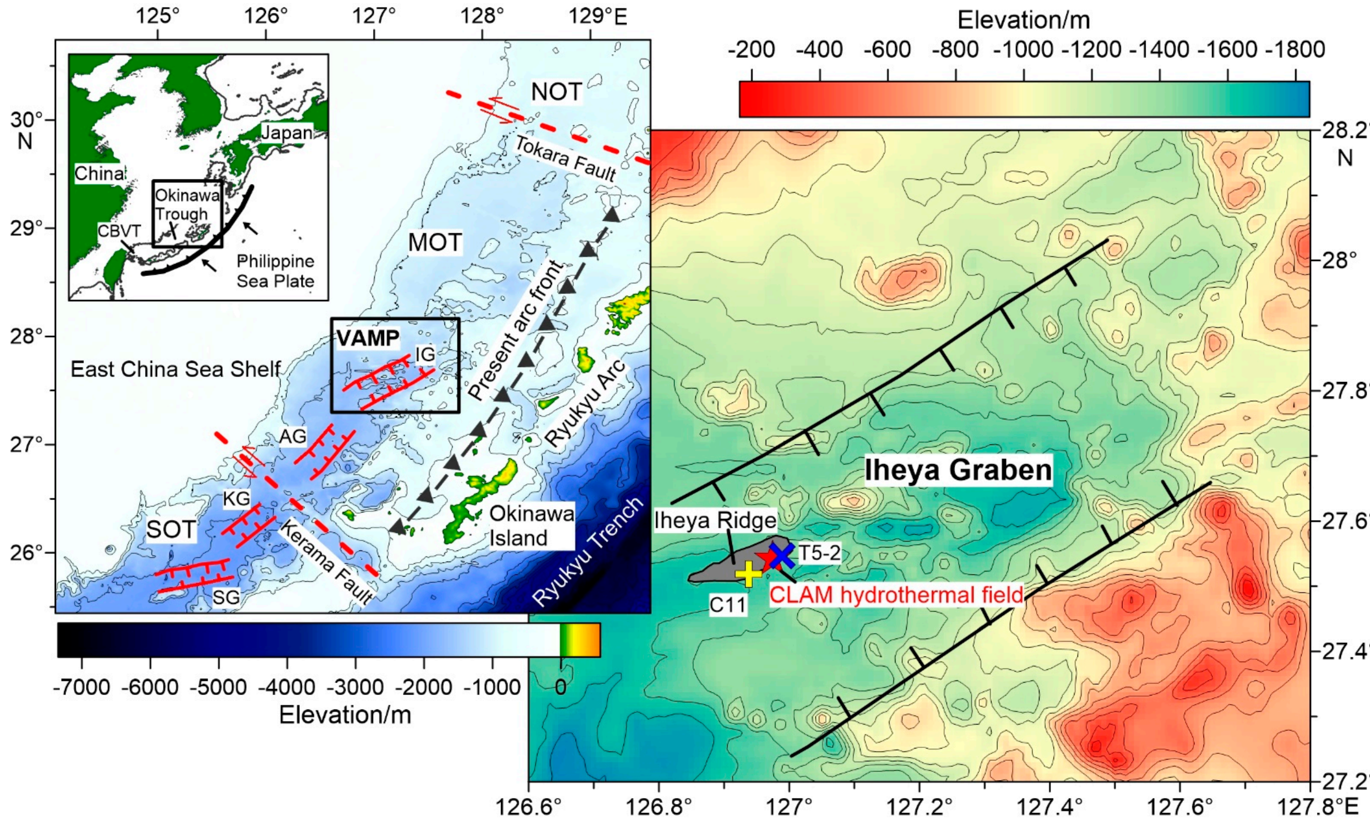

Figure 1. Bathymetric map of the Iheya Graben showing the locations of the Iheya Ridge (after [26]), samples (andesite T5-2 and rhyolite C11) and CLAM hydrothermal field. Abbreviations: NOT—northern Okinawa Trough; MOT—middle Okinawa Trough; SOT—southern Okinawa Trough. IG—Iheya Graben; AG—Aguni Graben, KG—Kerama Graben, and SG—Sakishima Graben.

The Iheya Ridge is a volcanic ridge located in the central axis of the Iheya Graben, which also represents the center of an anomalous volcanic zone (known as the VAMP area) (Figure 1). The volcanic rocks in the Iheya Ridge consist of basalts, andesites, and rhyolites. Multi-level magma storage and pervasive magma mixing are the key features of the magma plumbing system beneath this area [26]. An active hydrothermal field (CLAM) has been reported on the Iheya Ridge.

The samples used in this study included andesite (T5-2) and rhyolite (C11) collected from the Iheya Ridge. The detailed whole-rock geochemistry and mineralogical compositions of the Iheya Ridge have been reported previously [26]. Andesite T5-2 contains three groups of minerals that are in equilibrium with (1) rhyolitic melt, including low-Ca plagioclase, low-Mg orthopyroxene, and clinopyroxene with reverse zonations, (2) basaltic melt, including high-Ca plagioclase and high-Mg clinopyroxene with normal zonations, and (3) andesitic melt, including unzoned clinopyroxene and weakly zoned orthopyroxene (Figure S1). This indicates that the andesite used in this study was a mixture of basaltic and rhyolitic melts. Rhyolite C11 contains two groups of minerals that are in equilibrium with (1) host melt, including reversely zoned plagioclase and orthopyroxene, and (2) a less-evolved rhyolitic melt, including normally zoned plagioclase, unzoned orthopyroxene, and clinopyroxene (Figure S2). This suggests that the rhyolite used in this study was formed from a hybridization of rhyolitic melts with different evolution degrees.

3. Methods

We estimated the magma residence time from mixing to eruption beneath the Iheya Ridge using Mg diffusion in olivine, orthopyroxene, and plagioclase crystals. We chose olivine and reversely zoned orthopyroxene for andesite T5-2 and reversely zoned orthopyroxene and plagioclase and normally zoned plagioclase for rhyolite C11. These minerals all have euhedral crystal shapes, except for olivine (Figures 2 and 3). The olivine was corroded due to it mixing with rhyolitic melt (Figure 2a). No recrystallization of the olivine occurred because the hybrid andesitic melt destabilized the olivine. Instead, some tiny pigeonites were found to surround the olivine due to the reaction between olivine and rhyolitic melt (Figure 2a) [26].

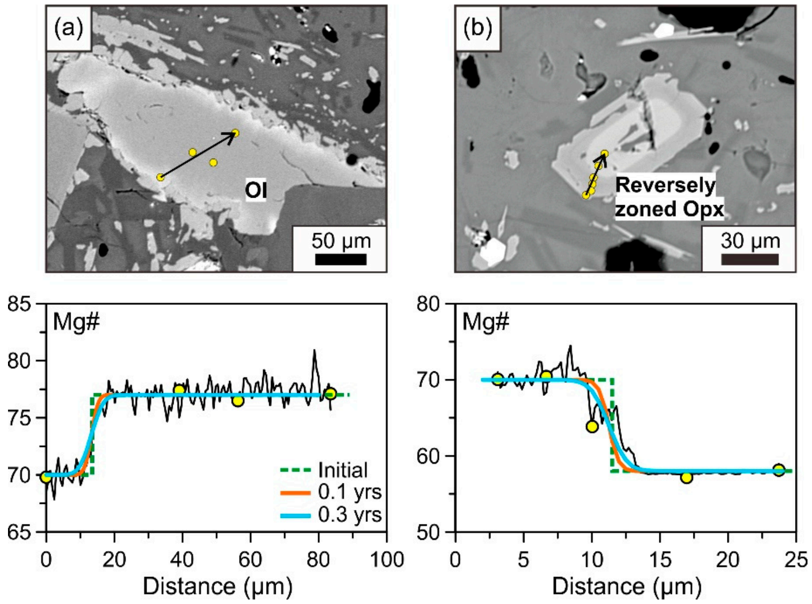

Figure 2. Modeling results of Mg diffusion in the olivine (**a**) and orthopyroxene (**b**) in andesite T5-2. The black curves were obtained from the gray values of BSE images. The yellow spots denote the data obtained by EMPA.

Because the Mg concentrations in olivine and orthopyroxene are proportional to the greyscale of the back-scattered electron (BSE) images of these minerals, the Mg profiles of the olivine and orthopyroxene in this study were calibrated from the greyscale values of high-resolution BSE images [29]. This method can obtain high-resolution Mg profiles. The BSE images were captured using an electron probe (EMPA) at the Ocean University of China under a beam current of 20 nA and at an accelerating voltage of 15 kV. The greyscale values of the BSE images were extracted using the ImageJ software. The greyscale values were then converted into Mg concentrations based on several (~4–6 points) EMPA analyses along the profiles. The Mg concentrations in the plagioclase were analyzed using laser ablation inductively coupled plasma mass spectrometry (LA-ICP-MS) at the State Key Laboratory of Isotope Geochemistry, Guangzhou Institute of Geochemistry, Chinese Academy of Sciences. The detailed analytical methods for EMPA and LA-ICP-MS are given in [26]. The analytical results are given in Data S1.

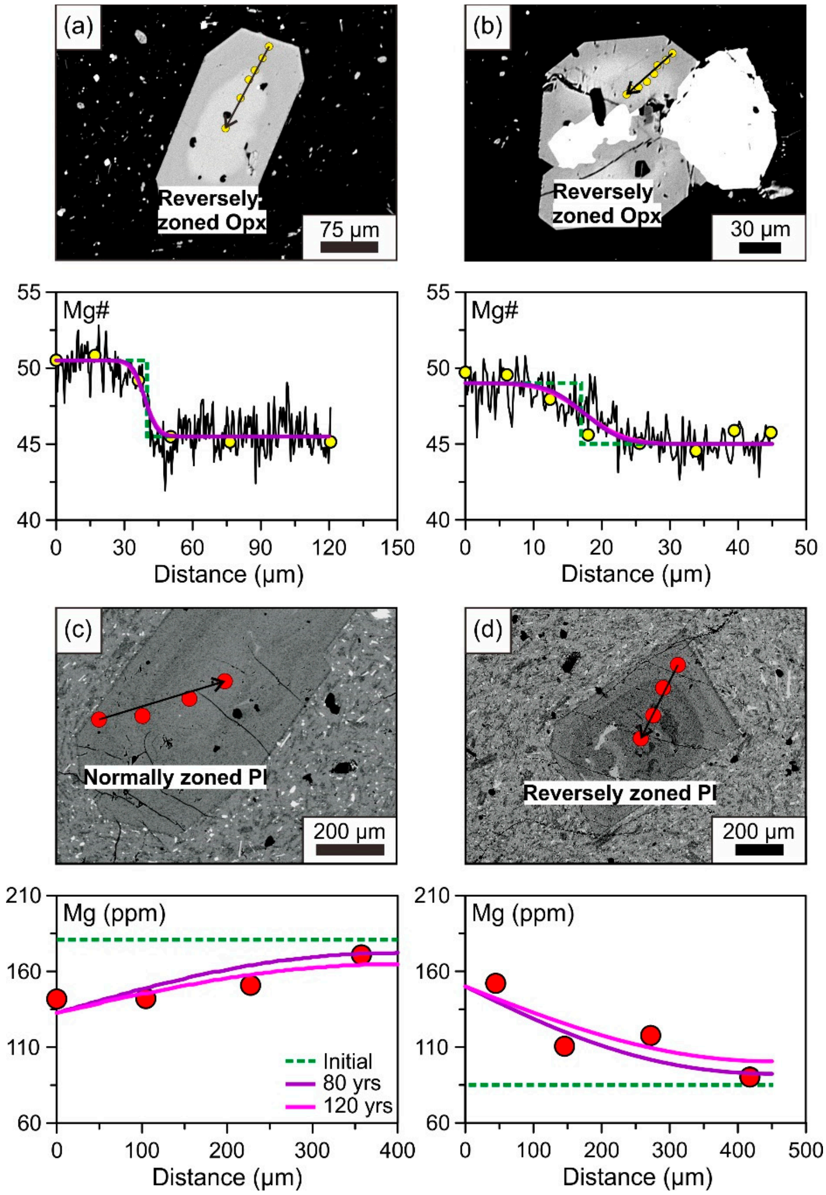

Figure 3. Modeling results of Mg diffusion in the orthopyroxene (**a**,**b**) and plagioclase (**c**,**d**) in rhyolite C11. The black curves in (**a**,**b**) were obtained from the gray values of BSE images. The yellow and red spots denote the data obtained by EMPA and LA-ICP-MS, respectively.

The Mg profiles of the crystals and their evolution with time can be modelled using the equation:

$$\partial C_i/\partial t = D_i \times \partial^2 C_i/\partial x^2 \quad (1)$$

where C_i and D_i represent the concentration and diffusion coefficient of the element i, respectively. The diffusion coefficients and P–T conditions used in the modelling are listed in Table 1. The crystal orientation was estimated according to the crystal shapes. Note that Mg diffusion in plagioclase is isotropic [30]. We assumed that the plagioclases had a homogeneous initial MgO concentration distribution. For the orthopyroxenes and olivines, we assumed that they had a homogeneous core with a higher/lower Mg# value surrounded by a homogeneous mantle with lower/higher Mg# value at the beginning of diffusion. The outermost rim compositions were used as the boundary conditions.

Table 1. Mg diffusion coefficients in olivine, orthopyroxene, and plagioclase.

	DMg ($\mu m^2/s$)	Orientation	P (kbar) [1]	T (°C) [1]	fO_2 (△NNO) [1]	X_{Mg}/X_{An}	Reference
Ol_T5-2	4.08×10^{-7}	[010]	2	970	−0.3	0.8	[31]
Opx_T5-2	6.22×10^{-8}	[001]	2	970	−0.3	\	[32]
Opx_C11	3.71×10^{-9}	[001]	2	870	−0.3	\	[32]
Pl_C11	1.11×10^{-5}	\	2	870	−0.3	0.35	[30]

[1] According to [26].

4. Results and Discussions

4.1. Timescales of Magma Mixing Beneath the Iheya Ridge

The diffusion modelling results are shown in Figures 2 and 3. In the andesite T5-2, the Mg diffusion in the olivine yielded a time of 0.1–0.3 years (Figure 2a). While the olivine crystal was slightly corroded, the Fe-rich rim had constant Mg# values, suggesting that the corrosion had little effect on the Mg diffusion profile across the Fe-rich and Mg-rich boundary. This time scale was quite consistent with that obtained from the Mg diffusion in orthopyroxene (0.1–0.3 years), which had an euhedral crystal shape (Figure 2b). In addition, the textures of the olivines in the T5-2 andesite (Figure 2a) were similar to those in the experiment of [33], where the olivines contacted with rhyodacitic and rhyolitic melt for up to 622 h at 800–885 °C and 50–150 MPa. This further suggested that the olivines in the andesite T5-2 contacted with the mixed magma for a very short time. In the rhyolite C11, the orthopyroxene crystals yielded a much longer magma residence time (80–120 years) (Figure 3a,b), which was consistent with the results calculated from the normally zoned plagioclase and the reversely zoned plagioclase (Figure 3c,d), although the latter were not well constrained due to the limited data.

It is noteworthy that the timescale calculation here was not a precise dating, as the diffusion coefficients were not constant but were dependent on the crystal compositions, crystal orientation, temperature, and so on [15,17,30–32]. Other uncertainties came from the choice of the initial and boundary conditions [17]. For example, the initial Mg concentrations of the plagioclases in the rhyolite C11 may not have been homogeneous. However, similar timescales yielded by multiple crystals indicated that our results were a plausible estimation.

Despite this uncertainty, our results suggested different magma residence times (from <1 year to ~100 years) beneath the Iheya Graben. The controlling factors on the timescales of magma mixing might be diverse, e.g., tectonic settings and the physical and chemical conditions of the magmas. Because the andesite T5-2 and rhyolite C11 used in this study were from the same location, their different magma residence times might be in part related to the different rheology and temperature of the mixed magmas. For example, rhyolite C11 is a mixture of rhyolitic melts [26], which have higher viscosities due to their higher SiO_2 concentrations and relatively lower temperatures. A high viscosity and a lower temperature would retard the magma flow and reduce the efficiency of magma mixing [34]. A long magma residence time (~600 year) was also reported in the southernmost part of the SOT, where the rhyolitic magma was intruded by small amount of basaltic magma (present as a mafic magma enclave) [25], suggesting inefficient magma mixing and a relatively high viscosity. In comparison, the andesite T5-2 in this study was generated by the mixing of a basaltic magma with a rhyolitic magma at a ratio of 4:6 [26]. The injection of a high proportion (40%) of high-temperature and low-SiO_2 basaltic magma would form a mixed magma with relatively low viscosity.

4.2. Rapid Magma Mixing and Eruption of Andesitic Magma in Bimodal Volcanic Series

The volcanic rocks in the OT are characterized by bimodal distributions, that is, basalts and rhyolites are dominant in the OT with scarce andesites [35–37]. The andesites have been suggested to have mainly been sourced from the mixing of basaltic magma with rhyolitic magma [26]. Therefore, the amount of andesites in the OT is probably dependent on the efficiency of magma mixing and eruption.

Magma mixing is considered to be an important trigger for eruptions [9,10]. An extremely short time between mixing and eruption has been reported (e.g., days to months) [21,38]. The short residence time (~0.1–0.3 years) of T5-2 magma after the magma mixing implied that the injection of basaltic magma into the rhyolitic magma may have led to the instability of the magma reservoir and the subsequent eruption. The efficient magma mixing suggested that the Iheya Ridge is a place that is favorable for the eruption of andesitic magma, which was consistent with the observation that the andesites recovered in the OT (excluding the modern arc fronts) so far were mostly from the Iheya Ridge and adjacent regions [26,36].

4.3. Implications for the Development and Preservation of Seafloor Hydrothermal Activities in the OT

The formation of seafloor hydrothermal activities involves the penetration of seawater into the crust, fluid–rock interactions heated by shallow magma, the rise of hydrothermal fluids, and the precipitation of hydrothermal products (e.g., sulfides), which may take from years to decades to occur [39]. Therefore, a long-term stable sub-seafloor magma system is essential for the development of a seafloor hydrothermal system with potential mineral resources. For example, the formation of a CLAM hydrothermal field on the Iheya Ridge might be attributed to a rhyolitic magma reservoir similar to that of C11 rhyolite. Similarly, long-term magma storage (~600 years) has also been reported near the Tangyin hydrothermal field [25]. However, the coexistence of a short magma storage suggests that the CLAM hydrothermal field may not have good prospects for resource exploitation because the rapid mixing and eruption could ruin the previously formed hydrothermal deposits and also present a great threat for mining activities. Therefore, evaluating the stability of sub-seafloor magmatic systems is a critical step in the assessment of seafloor hydrothermal resources.

5. Conclusions

The timescale of magma mixing beneath the Iheya Ridge was estimated by using Mg diffusion chronometry. The andesitic magma generated by the mixing between the basaltic and rhyolitic magmas experienced a very-short-time (~0.1–0.3 years) residence prior to eruption. In comparison, the rhyolitic magma generated by rhyolite–rhyolite mixing resided in the magma chamber for a much longer time (~80–120 years), which might have been in part related to the higher viscosity of the mixed magma. The rapid basalt–rhyolite mixing and eruption was favorable to the appearance of andesites in a bimodal volcanic series, but this is a disadvantage for the development and preservation of seafloor hydrothermal resources. This study thus emphasized the importance of evaluating the stability of sub-seafloor magma systems during the assessment of seafloor sulfide resources and mining prospects.

Supplementary Materials: The following supporting information can be downloaded at: https://www.mdpi.com/article/10.3390/jmse11020375/s1, Figure S1: Photomicrographs of three groups of minerals in andesite T5-2; Figure S2. Photomicrographs of two groups of minerals in rhyolite C11; Data S1: Mg concentrations of olivine, orthopyroxene, and plagioclase.

Author Contributions: Conceptualization, Y.Z.; methodology, Y.Z.; investigation, Y.Z.; resources, Z.Z.; data curation, Y.Z.; writing—original draft preparation, Y.Z.; writing—review and editing, Z.C. and Z.Z.; funding acquisition, Y.Z. and Z.Z. All authors have read and agreed to the published version of the manuscript.

Funding: This research was funded by the National Natural Science Foundation of China (91958213 and 42206058), the Strategic Priority Research Program (B) of Chinese Academy of Sciences (XDB42020402), the Shandong Provincial Natural Science Foundation, China (ZR2020QD068), and the Taishan Scholars Program.

Institutional Review Board Statement: Not applicable.

Informed Consent Statement: Not applicable.

Data Availability Statement: All the data that support the findings in this study are given in the Supporting Information or by contacting the corresponding authors.

Acknowledgments: We are grateful for the crew on the HOBAB4 cruise in 2016 for their help in collecting the samples.

Conflicts of Interest: The authors declare no conflict of interest.

References

1. Yang, K.; Scott, S.D. Possible contribution of a metal-rich magmatic fluid to a sea-floor hydrothermal system. *Nature* **1996**, *383*, 420–423. [CrossRef]
2. Ishibashi, J.I.; Urabe, T. Hydrothermal activity related to arc-backarc magmatism in the Western Pacific. In *Back Arc Basins*; Taylor, B., Ed.; Plenum Press: New York, NY, USA, 1995; pp. 451–495.
3. Butterfield, D.A.; Nakamura, K.-I.; Takano, B.; Lilley, M.D.; Lupton, J.E.; Resing, J.A.; Roe, K.K. High SO_2 flux, sulfur accumulation, and gas fractionation at an erupting submarine volcano. *Geology* **2011**, *39*, 803–806. [CrossRef]
4. Kienle, J.; Kowalik, Z.; Murty, T.S. Tsunamis generated by eruptions from Mount St. Augustine volcano, Alaska. *Science* **1987**, *236*, 1442–1447. [CrossRef] [PubMed]
5. McCoy, F.W.; Heiken, G. Tsunami Generated by the Late Bronze Age Eruption of Thera (Santorini), Greece. *Pure Appl. Geophys.* **2000**, *157*, 1227–1256. [CrossRef]
6. Esposito, A.; Giordano, G.; Anzidei, M. The 2002–2003 submarine gas eruption at Panarea volcano (Aeolian Islands, Italy): Volcanology of the seafloor and implications for the hazard scenario. *Mar. Geol.* **2006**, *227*, 119–134. [CrossRef]
7. Cashman, K.V.; Sparks, R.S.J.; Blundy, J.D. Vertically extensive and unstable magmatic systems: A unified view of igneous processes. *Science* **2017**, *355*, eaag3055. [CrossRef]
8. Geiger, H.; Troll, V.R.; Jolis, E.M.; Deegan, F.M.; Harris, C.; Hilton, D.R.; Freda, C. Multi-level magma plumbing at Agung and Batur volcanoes increases risk of hazardous eruptions. *Sci. Rep.* **2018**, *8*, 10547. [CrossRef]
9. Murphy, M.D.; Sparks, R.S.J.; Barclay, J.; Carroll, M.R.; Lejeune, A.M.; Brewer, T.S.; Macdonald, R.; Black, S.; Young, S. The role of magma mixing in triggering the current eruption at the Soufriere Hills Volcano, Montserrat, West Indies. *Geophys. Res. Lett.* **1998**, *25*, 3433–3436. [CrossRef]
10. Sparks, S.R.J.; Sigurdsson, H.; Wilson, L. Magma mixing: A mechanism for triggering acid explosive eruptions. *Nature* **1977**, *267*, 315–318. [CrossRef]
11. Kahl, M.; Chakraborty, S.; Costa, F.; Pompilio, M. Dynamic plumbing system beneath volcanoes revealed by kinetic modeling, and the connection to monitoring data: An example from Mt. Etna. *Earth Planet Sci. Lett.* **2011**, *308*, 11–22. [CrossRef]
12. Kahl, M.; Chakraborty, S.; Pompilio, M.; Costa, F. Constraints on the Nature and Evolution of the Magma Plumbing System of Mt. Etna Volcano (1991–2008) from a Combined Thermodynamic and Kinetic Modelling of the Compositional Record of Minerals. *J. Petrol.* **2015**, *56*, 2025–2068. [CrossRef]
13. Albert, H.; Costa, F.; Martí, J. Timing of magmatic processes and unrest associated with mafic historical monogenetic eruptions in Tenerife Island. *J. Petrol.* **2015**, *56*, 1945–1966. [CrossRef]
14. Cooper, G.F.; Morgan, D.J.; Wilson, C.J.N. Rapid assembly and rejuvenation of a large silicic magmatic system: Insights from mineral diffusive profiles in the Kidnappers and Rocky Hill deposits, New Zealand. *Earth Planet Sci. Lett.* **2017**, *473*, 1–13. [CrossRef]
15. Costa, F.; Chakraborty, S.; Dohmen, R. Diffusion coupling between trace and major elements and a model for calculation of magma residence times using plagioclase. *Geochim. Cosmochim. Acta* **2003**, *67*, 2189–2200. [CrossRef]
16. Costa, F.; Coogan, L.A.; Chakraborty, S. The time scales of magma mixing and mingling involving primitive melts and melt–mush interaction at mid-ocean ridges. *Contrib. Mineral. Petrol.* **2010**, *159*, 371–387. [CrossRef]
17. Costa, F.; Dohmen, R.; Chakraborty, S. Time scales of magmatic processes from modeling the zoning patterns of crystals. *Rev. Mineral. Geochem.* **2008**, *69*, 545–594. [CrossRef]
18. Lynn, K.J.; Garcia, M.O.; Shea, T.; Costa, F.; Swanson, D.A. Timescales of mixing and storage for Keanakāko'i Tephra magmas (1500–1820 C.E.), Kīlauea Volcano, Hawai'i. *Contrib. Mineral. Petrol.* **2017**, *172*, 76. [CrossRef]
19. Nishi, Y.; Ban, M.; Takebe, M.; Álvarez-Valero, A.M.; Oikawa, T.; Yamasaki, S. Structure of the shallow magma chamber of the active volcano Mt. Zao, NE Japan: Implications for its eruptive time scales. *J. Volcanol. Geotherm. Res.* **2019**, *371*, 137–161. [CrossRef]

20. Petrone, C.M.; Braschi, E.; Francalanci, L.; Casalini, M.; Tommasini, S. Rapid mixing and short storage timescale in the magma dynamics of a steady-state volcano. *Earth Planet Sci. Lett.* **2018**, *492*, 206–221. [CrossRef]
21. Tomiya, A.; Miyagi, I.; Saito, G.; Geshi, N. Short time scales of magma-mixing processes prior to the 2011 eruption of Shinmoedake volcano, Kirishima volcanic group, Japan. *Bull. Volcanol.* **2013**, *75*, 750. [CrossRef]
22. Glasby, G.P.; Notsu, K. Submarine hydrothermal mineralization in the Okinawa Trough, SW of Japan: An overview. *Ore Geol. Rev.* **2003**, *23*, 299–339. [CrossRef]
23. Sibuet, J.C.; Deffontaines, B.; Hsu, S.K.; Thareau, N.; Formal, L.; Liu, C.S. Okinawa Trough backarc basin: Early tectonic and magmatic evolution. *J. Geophys. Res. Solid Earth* **1998**, *103*, 30245–30267. [CrossRef]
24. Zhang, L.; Luan, X.; Zeng, Z.; Liu, H. Key parameters of the structure and evolution of the Okinawa Trough: Modelling results constrained by heat flow observations. *Geol. J.* **2019**, *54*, 3542–3555. [CrossRef]
25. Chen, Z.; Zeng, Z.; Wang, X.; Peng, X.; Zhang, Y.; Yin, X.; Chen, S.; Zhang, L.; Qi, H. Element and Sr isotope zoning in plagioclase in the dacites from the southwestern Okinawa Trough: Insights into magma mixing processes and time scales. *Lithos* **2020**, *376–377*, 105776. [CrossRef]
26. Zhang, Y.; Zeng, Z.; Gaetani, G.; Zhang, L.; Lai, Z. Mineralogical constraints on the magma mixing beneath the iheya graben, an active back-arc spreading center of the Okinawa trough. *J. Petrol.* **2020**, *61*, egaa098. [CrossRef]
27. Sibuet, J.C.; Letouzey, J.; Barbier, F.; Charvet, J.; Foucher, J.P.; Hilde, T.W.; Kimura, M.; Chiao, L.Y.; Marsset, B.; Muller, C. Back arc extension in the Okinawa Trough. *J. Geophys. Res. Solid Earth* **1987**, *92*, 14041–14063. [CrossRef]
28. Zhang, Y.; Zeng, Z.; Wang, X.; Chen, S.; Yin, X.; Chen, Z. Geologic control on hydrothermal activities in the Okinawa Trough. *Adv. Earth Sci.* **2020**, *35*, 678–690.
29. Fabbro, G.N.; Druitt, T.H.; Costa, F. Storage and Eruption of Silicic Magma across the Transition from Dominantly Effusive to Caldera-forming States at an Arc Volcano (Santorini, Greece). *J. Petrol.* **2017**, *58*, 2429–2464. [CrossRef]
30. Van Orman, J.A.; Cherniak, D.J.; Kita, N.T. Magnesium diffusion in plagioclase: Dependence on composition, and implications for thermal resetting of the ^{26}Al–^{26}Mg early solar system chronometer. *Earth Planet Sci. Lett.* **2014**, *385*, 79–88. [CrossRef]
31. Dohmen, R.; Chakraborty, S. Fe–Mg diffusion in olivine II: Point defect chemistry, change of diffusion mechanisms and a model for calculation of diffusion coefficients in natural olivine. *Phys. Chem. Miner.* **2007**, *34*, 409–430. [CrossRef]
32. Dohmen, R.; Ter Heege, J.H.; Chakraborty, S.; Becker, H.-W. Fe-Mg interdiffusion in orthopyroxene. *Am. Mineral.* **2016**, *101*, 2210–2221. [CrossRef]
33. Coombs, M.L.; Gardner, J.E. Reaction rim growth on olivine in silicic melts: Implications for magma mixing. *Am. Mineral.* **2004**, *89*, 748–758. [CrossRef]
34. Laumonier, M.; Scaillet, B.; Pichavant, M.; Champallier, R.; Andujar, J.; Arbaret, L. On the conditions of magma mixing and its bearing on andesite production in the crust. *Nat. Commun.* **2014**, *5*, 5607. [CrossRef]
35. Shinjo, R.; Chung, S.L.; Kato, Y.; Kimura, M. Geochemical and Sr-Nd isotopic characteristics of volcanic rocks from the Okinawa Trough and Ryukyu Arc: Implications for the evolution of a young, intracontinental back arc basin. *J. Geophys. Res. Solid Earth* **1999**, *104*, 10591–10608. [CrossRef]
36. Shinjo, R.; Kato, Y. Geochemical constraints on the origin of bimodal magmatism at the Okinawa Trough, an incipient back-arc basin. *Lithos* **2000**, *54*, 117–137. [CrossRef]
37. Zhang, Y.; Zeng, Z.; Chen, S.; Wang, X.; Yin, X. New insights into the origin of the bimodal volcanism in the middle Okinawa Trough: Not a basalt-rhyolite differentiation process. *Front. Earth Sci.* **2018**, *12*, 325–338. [CrossRef]
38. Siegburg, M.; Klügel, A.; Rocholl, A.; Bach, W. Magma plumbing and hybrid magma formation at an active back-arc basin volcano: North Su, eastern Manus basin. *J. Volcanol. Geotherm. Res.* **2018**, *362*, 1–16. [CrossRef]
39. Alt, J.C. Subseafloor processes in mid-ocean ridge hydrothennal systems. In *Seafloor Hydrothermal Systems: Physical, Chemical, Biological, and Geological Interactions*; Humphris, S.E., Zierenberg, R.A., Mullineaux, L.S., Thomson, R.E., Eds.; American Geophysical Union: Washington, WA, USA, 1995; pp. 85–114.